Effect of Tensile Reinforcement Ratio on the Effective Moment of Inertia of Reinforced Lightweight Concrete Beams for Short Term Deflection Calculation

Akmaluddin

Faculty of Engineering, University of Mataram, Mataram, Indonesia
Email: akmal2k4@yahoo.co.uk

Abstract. This paper presents an improvement model of the effective moment of inertia to predict the short term deflection of reinforced lightweight concrete beam. The models were developed using 9 beams of reinforced pumice-lightweight concrete tested under two symmetrical-point loads. The presence of steel reinforcement in the beam was taken into consideration in the developed model. The models were verified by test carried out on other 9 beams. Those beams subjected to various-point loads and compressive strength. The results of investigation revealed that crack moment of inertia increased with the increased tensile reinforcement ratio. Thus, the reinforcement ratio significantly affects the value of effective moment of inertia of reinforced lightweight concrete beam. All the beam test results produced considerable deflection in comparison to that obtained using current Codes either ACI or SNI. The proposed model demonstrated a good agreement to the experimental results and in some cases have similar trend to that of the ACI or SNI prediction.

Keywords: *Effective moment of inertia; lightweight reinforced concrete; beam deflection.*

1 Introduction

Lombok Island is one of the islands of the Indonesian archipelago which has the volcano. Hence, there is a lot of pumice in this area as one of its natural resources. Pumices with relatively large size are highly demanded to be exported, but not so with the small one. This material is categorized as solid waste. This waste is normally disposed around the area of sorting places carelessly leading to the damage of the environment. Therefore, using this waste as sustainable building material in the construction industry helps to preserve natural resources and environmental pollution. As pumice is a natural material of volcanic origin produced by the release of gases during the solidification of lava therefore, in nature it is quite hard and does not deteriorate easily once bound in concrete. The bulk density of pumices varies from 400 to 600 kg/m^3, producing concretes density of about 1850 kg/m^3, which makes them lightweight. It has been found that pumice concrete can reach the strength of 17

Received November 2nd, 2010, Revised May 11th, 2011, Accepted for publication June 21st, 2011.
 ISSN: 1978-3051, DOI: 10.5614/itbj.eng.sci.2011.43.3.4

MPa [1] which is a minimum requirement for structural lightweight concrete as per ASTM C330 [2] or SNI 03-2847 [3].

Many attempts have been made to study various natural and artificial materials to make lightweight aggregate as material of lightweight concrete component for building construction. Researchers [4,5] have studied and modified these materials to obtain material with low density, high strength and durability. Owens [6] indicated that structural lightweight concrete have excellent prospect as an alternative construction element. It is because of lightweight concrete has sufficient strength structurally and it also has low density that can reduce self-weight significantly in building structure. He also concluded that replacing the normal-weight concrete with lightweight concrete is economically advantageous.

2 Effective Moment of Inertia in the Current Code of Practice

Since 1970s American Standard has introduced formula for calculating the effective moment of inertia of beam deflection [7]. The formula was proposed in 1963 by Branson [8] as given by Eq. (1). This equation also adopted by Indonesia's current code [3].

$$I_e = I_g \left(\frac{M_{cr}}{M_a} \right)^3 + I_{cr} \left\{ 1 - \left(\frac{M_{cr}}{M_a} \right)^3 \right\} \tag{1}$$

where, I_g is gross moment of inertia ignoring reinforcement, I_{cr} is cracking moment of inertia. In the case of rectangular section with tension reinforcement only, I_g and I_{cr} are given by Eq. (2), and Eq. (3) respectively. M_a is service moment and M_{cr} is first cracking moment as shown in Eq. (4).

$$I_g = \frac{1}{12} bh^3 \tag{2}$$

$$I_{cr} = \frac{1}{3} bc^3 + nA_s (d - c)^2 \quad \text{with } c = kd \text{ and } k = \sqrt{(n\rho)^2 + 2n\rho} - n\rho \tag{3}$$

$$M_{cr} = \frac{f_r \, I_g}{y_t} \tag{4}$$

where *b*, *h* and *d* are representation of breadth, height and effective depth of the beam respectively. Whilst, *n* is modular ratio and ρ is tensile reinforcement ratio defined as A_s/bd with A_s is total area of steel.

Many researchers [9-15] have studied beam deflection to improve the equation. The new finding formula as possible replacement for the equation was introduced in 1998 [16] and modified recently by the author on the I_{cr} and factor Φ [17] for rectangular section with tension reinforcement only as given in Eqs. (6) and (7) respectively.

$$I_e = I_{cr} + (I_g - I_{cr})e^{\Phi} \tag{5}$$

with

$$I_{cr} = (0.1618 + 0.0418\ n\rho)\tfrac{1}{12}bd^3 \tag{6}$$

$$\Phi = -\left(\frac{M_a}{M_{cr}}\right)\left(\frac{L_{cr}}{L}\right)(8.474 - 9.0607\rho + 2.842\rho^2) \tag{7}$$

where L_{cr}/L is theoretically depend on the loading condition acting on the beam. This will be presented clearly later on.

The above equation, however, was purely generated from normal weight concrete beams specimens. The use of lightweight concrete beams as structural elements for building construction in the future has got the attention of many researchers [18,19]. But the attention given has not been accompanied by studying improvement model for analyzing the beam, especially for short-term deflection calculation as one of serviceability requirements. Therefore this study specifically aims to examine and improve the effective moment of inertia model used for the normal-weight concrete beam as given by Eqs. (6) and (7) above so as to be valid for predicting the deflection of lightweight concrete beams.

3 Experimental Program

3.1 Material and Mix Proportions

Concrete mix design to produce concrete with three different grades considered was made for the purpose of current investigation. Pumice was used as full replacement for the natural gravel in the manufacture of lightweight concrete. Table 1 shows the properties of aggregate used in this investigation.

The materials used in the mix were ordinary portland cement (Type I with trade mark of Tiga Roda), pumice, sand and silica fume of Sica™ production. Using

the above aggregate the mix proportions were designed as given in Table 2 for the variation strength considered in this study.

Table 1 Aggregate properties.

Properties	Pumice	Sand
Maximum aggregate size (mm)	12.5	-
Bulk density (kg/m^3)	486	1702
Unit weight (SSD) (gr/cm^3)	0.452	1.471
Fineness modulus	6.483	4.92
Mud content (%)	-	0.86
Water absorption (%)	38.87	1.58
Water content (%)	41.93	13.33
Specific gravity (SSD)	1.24	2.74

Table 2 Mix proportions for 1 m^3 lightweight concrete.

f'_c (MPa)	W/C	PC (kg)	Water (kg)	Pumice (kg)	Sand (kg)	Silica Fume (kg)
17	0.4	507.50	203.00	382.28	467.23	-
20	0.3	676.67	203.00	272.13	408.20	-
25	0.3+SF	676.67	203.00	275.70	336.97	67.67

3.2 Reinforced Concrete Beam Details

A total of 18 beams were fabricated and tested at the age of 28 days. The beams were divided into 3 series. Series B1, B2 and B3 are referred to as the beams subjected to symmetrical, asymmetrical two-point loads and single-point load respectively. These load variation were considered as representation of factor (L_{cr}/L) in the Eq.(7). The details of beams used and its designation are shown in Table 3. Number 17, 20 and 25 in the table presents compressive strength of 17, 20 and 25 MPa respectively. Three reinforcement ratios of 0.72%, 1.08% and 1.80% were used as representation for low (L), normal (N) and high (H) reinforcement respectively. The main tensile reinforcement was a plane bar with diameter of 12 mm and it had yield strength, f_y = 250 N/mm^2 and elastic modulus E_s = 200 kN/mm^2. The compression reinforcement and stirrups were 6 mm steel plane bar which had the same properties as the main tensile reinforcement and the stirrup were placed at 130 mm along the length of the span. Accompanying the beam test, the required number of cylinders was tested on the same day as the beam testing to determine the properties of the concrete. Schematic test set-up, geometry and detail reinforcement are shown in Figure 1.

Table 3 Load arrangement and beams designation.

Series	Load Condition	ρ = As/*bd* (%) Low (L)	Normal (N)	High (H)	f'_c (MPa)	Designation		
B1	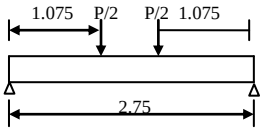	0.72	1.08	1.80	17	B1L17	B1N17	B1H17
					20	B1L20	B1N20	B1H20
					25	B1L25	B1N25	B1H25
B2	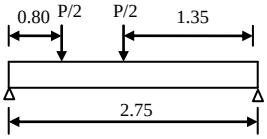	0.72	1.08	1.80	17	B2L17	B2N17	B2H17
					20	B2L20	B2N20	B2H20
B3	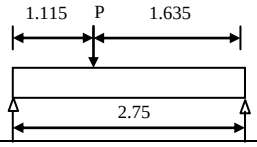	0.72	1.08	1.80	25	B3L25	B3N25	B3H25

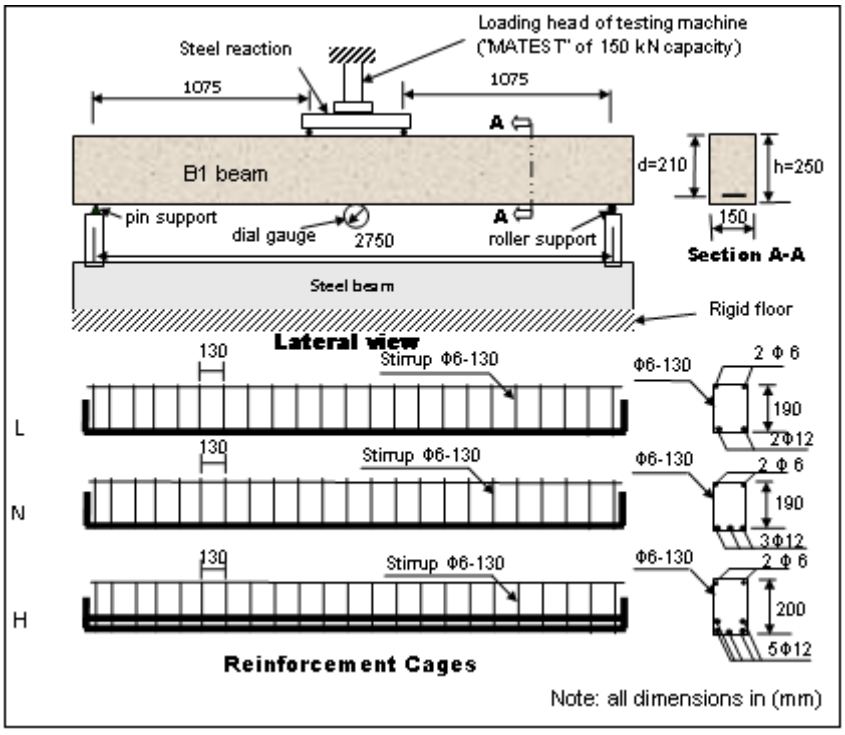

Figure 1 Schematic drawing showing test set-up and reinforcement configuration.

3.3 Fabrication and Casting

For casting the beam specimen, formwork was cleaned and placed on the flat floor. The steel cages prepared was inserted into the formwork and stood to make 40 mm concrete cover. The concrete was then poured to form and compacted by vibration. Three test cylinders were prepared at the same time as the concrete was poured. The beam specimens were covered with wet burlap and plastic sheeting. Water was sprinkled twice a day to keep the specimens moist. The formwork was dismantled seven days after concrete pouring and the specimens left to cure under ambient conditions.

3.4 Test Setup and Procedures

The beams were tested in the Laboratory of Structure and Material, Faculty of Engineering, University of Mataram. A "MATEST" flexural testing machine of 150 kN capacity with 0.5 kN accuracy was applied. The beams of 3 m length were simply supported with clear span of 2.75 m. A "Mitutoyo" dial gauge reading of 50 mm was used to measure deflection. The dial gauge was placed at the beam mid span. The load was given incrementally and kept constant at loading rate of about 0.018 mm/sec.

All the beams series described in Table 3 were tested until failure in flexure. Testing series B1 were conducted in advance to develop model, then followed by testing the B2 and B3 beams series for verifying the model. Prior to the testing started, each beam specimen was painted white so that crack patterns could be easily observed. The specimen was then placed in the loading frame in the correct position. The dial gauge of 0.01 mm accuracy was placed in the mid span of the beam to monitor deflection. A small load of around 1 kN was first applied to make sure that all the instruments were working. The load was then increased gradually with an increment of approximately 3 kN. During the test, the load at each stage was kept constant for a while to allow the observation of the crack development in the beam surface and to read the deflection. The cracks were marked both on the left and right side of the beam with given number indicating the corresponding load. The general behaviour of the specimen was carefully observed during the load application. The load was terminated after the beam failure. The failure load was then identified when excessive cracking occurs at the bottom of the beam and the applied load drops simultaneously with the deflection increased. In addition, ASTM C39-86 [20] and ASTM C-469 [21] were adopted for testing compressive strength and elastic modulus of concrete respectively.

4 Results

4.1 Beam Properties

The cylinder test results produced compressive strength of 19.05 MPa, 22.26 MPa and 26.6 MPa for compressive strength set of 17, 20 and 25 MPa respectively. This results in line with expectation. And also concrete modulus of elasticity of 12600, 13800, 15700 MPa were obtained for 17, 20 and 25 MPa concrete compressive strength respectively. These results are close to 65% of ordinary concrete modulus of elasticity as expected for lightweight concrete.

4.2 Behaviour of the Beam Test Specimens

When reinforced concrete beam is loaded the beam will deflect and crack(s) occur. With the cracks in the beam, the beam stiffness is reduced as indicated by the change of line direction on curve as can be seen at point A in Figure 2. This point namely crack moment, M_{cr}, which is defined as the moment that produces the first crack(s) in the beam surfaces. This can be seen as a point on the moment-deflection curve at which the form of the curve becomes nonlinear [11].

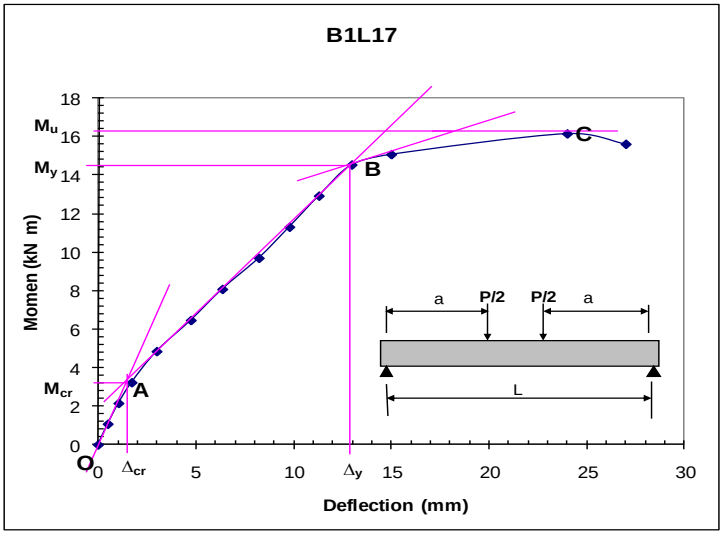

Figure 2 Moment-deflection curve for analysing M_{cr}, M_y and $M_{u.}$

With the load is increased the beam stiffness decreased until reach minimum stiffness, I_{cr}. This indicates that the beam section is fully crack, produce a further change in shape occurs at point B. At this load level, the steel reinforcement is yielding thus this load is called M_y [11]. The slope at the curve then changes gradually until point C is reached. At this point, a plastic hinge is

formed in the concrete beam and very little further increment in load can be achieved so the load is maximum then called as ultimate load, P_u or M_u when the ultimate load is multiplied by shear span, a. In order to evaluate $M_{cr(exp)}$, the beam behaviour above was adopted where the moment-deflection curve was simplified to three linier portions OA, AB and BC where the two lines OA and AB intersected the moment value was taken as $M_{cr(exp)}$. Similarly, intersection line between AB and BC was taken as M_y and point C was taken as M_u. These moments corresponding to deflection Δ_{cr}, Δ_y, and Δ_u as can be seen in Figure 2. The technique adopted above is more convenient which give sufficient results in terms of M_y evaluation instead of using moment-curvature relationship that need strain measurement of concrete and tensile reinforcement of the beam [22].

4.3 Experimental Moments

Using procedure described in section 4.2 above then the experimental value of M_{cr}, M_y and M_u for other beam specimens are presented in Table 4. It can be seen that first cracking moment, M_{cr}, has varying value from 0.2 to 0.33 against maximum moment, M_u. Whilst, ratio yield moments, M_y, against M_u have value between 0.82 and 0.94.

Table 4 Moments obtained experimentally.

Beam Specimens	M_{cr} (kNm)	Δ_{cr} (mm)	M_y (kNm)	Δ_y (mm)	M_u (kNm)	Δ_u (mm)	M_{cr}/M_u	M_y/M_u
(1)	(2)	(3)	(4)	(5)	(6)	(7)	(8)=(2/6)	(9)=(4/6)
B1L17	3.25	1.72	14.51	12.00	16.00	16.20	0.20	0.91
B1N17	5.60	2.46	19.35	12.75	22.80	23.00	0.25	0.85
B1H17	6.45	3.34	25.80	16.00	29.60	29.00	0.22	0.87
B1L20	4.84	1.96	14.51	11.00	16.00	16.00	0.30	0.91
B1N20	6.45	2.55	21.50	13.50	22.85	22.80	0.28	0.94
B1H20	9.68	4.74	26.88	16.20	32.80	32.50	0.30	0.82
B1L25	4.84	2.85	15.05	10.50	16.50	15.20	0.29	0.91
B1N25	6.45	2.68	22.04	12.50	25.26	25.00	0.26	0.87
B1H25	11.28	5.4	30.00	16.00	34.67	26.70	0.33	0.87

The first crack moment values obtained above shows that its value depends on the amount of reinforcement and compressive strength in the beam. The more reinforcement given, the greater M_{cr} value is. By considering the theoretical M_{cr} value given by equation (4) depends on the geometry and strength of concrete only, then to simplify the formula in the development model, the effect of reinforcement is not taken into consideration in the M_{cr} formula. This means that Eq. (4) is still valid.

4.4 Model Improvement

Similar to the authors' previous study, procedures to improve the model were still adopted. The data obtained from B1 beams test result were used to build the model improvement and verify to the beam subjected to asymmetrical point(s) load as denoted by beams B2 and B3 for asymmetrical two points load and single point load at any position respectively.

4.4.1 Modification of I_{cr}

Deflection at mid span for each beam with two symmetrical points load is calculated using the following equation.

$$\Delta = \frac{M_a\left(3L^2 - 4a^2\right)}{24E_c I} \qquad \text{(mm)} \tag{8}$$

where M_a is the moment acting on the beam (N mm), a is the distance between load position and support (mm), E_c is the elastic modulus of concrete (MPa), L represent span length of the beam (mm) and I is moment of Inertia (mm^4). As the concrete beam is cracking when loaded then I is not constant thus it is replaced by the term I_e giving effective value of moment of inertia of the beam. Experimentally, deflection can be measured accurately. When the experimental value is substituted into Eq. (8) then experimental I_e could be worked out as given by Eq. (9) below.

$$I_{e(\exp)} = \frac{M_a\left(3L^2 - 4a^2\right)}{24E_c\Delta_{\exp}} \qquad (\text{mm}^4) \tag{9}$$

When the load acting less than cracking load ($M_a<M_{cr}$), the section is uncracked [11] therefore $I_e=I_g$. However, by increasing the load until reach the yield load ($M_a=M_y$), the section is fully cracked thus $I_e=I_{cr}$. For this reason $I_{e(exp)} = I_{cr(exp)}$, therefore Eq. (9) can be modified to obtain the experimental values of I_{cr} as Eq. (10).

$$I_{cr(\exp)} = \frac{M_y\left(3L^2 - 4a^2\right)}{24E_c\Delta_{\exp}} \qquad (\text{mm}^4) \tag{10}$$

In all test beam results, the ratios between experimental and theoretical crack moment of inertia are below unity. It can be seen from Table 5 that at different compressive strength, the ratio of experimental to analytical cracking moment of inertia decreased with increasing reinforcement ratio as shown in column (6) of Table 5. This variation suggests that factor compressive strength, f'_c, and

reinforcement ratio, ρ, affect the value. By referring to Eq. (3) the term $n\rho$ is adopted, therefore, parameter f'_c is not taken into consideration to relate directly with cracking moment of inertia. The n parameter represent modular ratio of the beam section meaning that the parameter relies on elastic modulus of steel, E_s, and concrete modulus of elasticity, E_c. Since the E_c is function of f'_c, thus parameter n is assumed to be representation of f'_c indirectly. Hence, using the term $n\rho$ instead of f'_c and ρ in the proposed equation of cracking moment of inertia is preferred.

Table 5 Observation and analysis crack moment of inertia.

Beam Designation	M_y **(kN m)**	Δ_y **(mm)**	$I_{cr(exp)}$ **(mm^4)**	$I_{cr\ (th)}$ **(mm^4)**	**Ratio (4)/(5)**
(1)	(2)	(3)	(4)	(5)	(6)
B1L17	14.51	12.00	7.23E+07	8.63E+07	0.84
B1N17	19.35	12.75	9.07E+07	1.14E+08	0.80
B1H17	25.80	16.00	9.64E+07	1.56E+08	0.62
B1L20	14.51	11.00	7.27E+07	8.14E+07	0.89
B1N20	21.50	13.50	8.77E+07	1.08E+08	0.81
B1H20	26.88	16.20	9.14E+07	1.49E+08	0.61
B1L25	15.05	10.50	7.06E+07	7.50E+07	0.94
B1N25	22.04	12.50	8.69E+07	1.00E+08	0.87
B1H25	30.00	16.00	8.77E+07	1.39E+08	0.63

Therefore, after several times of trying, the best possibility was by plotting average ratio $I_{cr(\exp)} \Big/ \frac{1}{12} bd^3$ against $(n\rho)^{0.25}$ as shown in Figure 3.

By applying linear trend line to the data in the figure it will give the best fit of the data and produce alternative for I_{cr}. Using regression analysis this produces new cracking moment of inertia, I_{crn} as given by Eq. (11) below.

$$I_{crn} = 0.36\ (n\rho)^{0.25} \times \tfrac{1}{12} bd^3 \quad (\text{mm}^4) \tag{11}$$

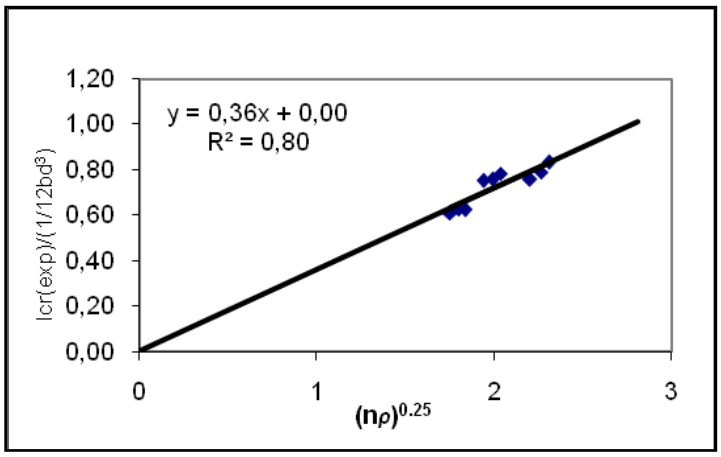

Figure 3 Regression analysis to obtain Eq. (11).

4.4.2 Modification of Factor Φ

Experimental value of factor Φ was obtained by rearranging Eq. (5) and replace I_e with $I_{e(exp)}$ and used I_{crn} instead of I_{cr} gives results as Eq. (12).

$$\Phi_{\exp} = \ln\left|\frac{I_{e(\exp)} - I_{crn}}{I_g - I_{crn}}\right| \tag{12}$$

Substitute Eq. (9) into Eq. (12) to obtain experimental Φ values. The Φ values divided by $\left(M_a/M_{cr}\right)\left(L_{cr}/L\right)$ were defined as C and their average value are plotted against reinforcement ratio as shown in Figure 4. From regression analysis this produce Eq. (13).

$$\Phi_n = -\left(\frac{M_a}{M_{cr}}\right)\left(\frac{L_{cr}}{L}\right)(1.41 + 0.44\rho) \tag{13}$$

L_{cr}/L in the Eq. (13) is function of loading condition [10]. For more convenient, the formula of L_{cr}/L for each load condition is presented. Eq. (14) is used to obtain the L_{cr}/L value for two symmetrical points load.

$$\frac{L_{cr}}{L} = 1 - \frac{M_{cr}}{M_a}\left(\frac{2a}{L}\right) \tag{14}$$

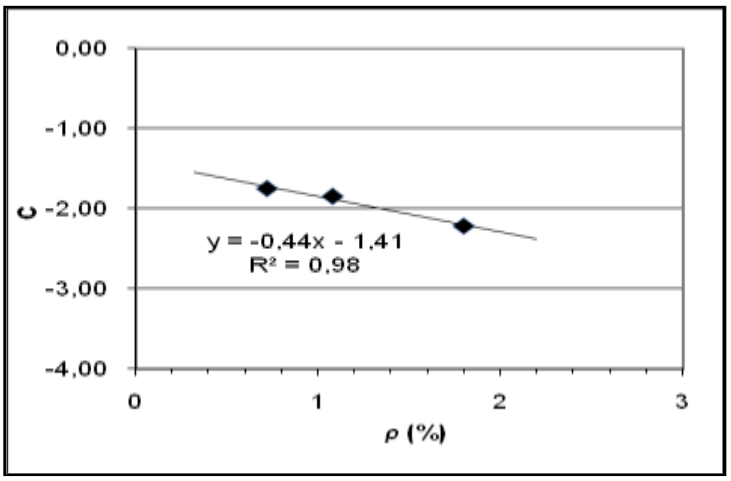

Figure 4 Regression analysis for the factor Φ.

For two asymmetrical points load the value of L_{cr}/L is obtained using Eq. (15) and for the single point load at any position the value can be calculated using Eq. (16).

$$\frac{L_{cr}}{L} = 1 - \frac{M_{cr}}{M_a}\left(\frac{a}{L} + \frac{b}{L}\frac{M_a}{M_b}\right) \tag{15}$$

$$\frac{L_{cr}}{L} = 1 - \frac{M_{cr}}{M_a} \tag{16}$$

At last, by substituting the appropriate value of L_{cr}/L into Eq. (13) gives the formula Φ for each loading type. These values are presented in Eqs. (17), (18) and (19) for symmetrical two points load, asymmetrical two points and single point load respectively.

$$\Phi = -\left[\frac{M_a}{M_{cr}} - 2\frac{a}{L}\right](1.41 + 0.44\rho) \tag{17}$$

$$\Phi = -\left[\frac{M_a}{M_{cr}} - \frac{a+b}{L}\frac{M_a}{M_b}\right](1.41 + 0.44\rho) \tag{18}$$

$$\Phi = -\left[\frac{M_a}{M_{cr}} - 1\right](1.41 + 0.44\rho) \tag{19}$$

Parameter *a* and *b* in all the equations above represent distance between support and load position, where smaller value always taken as *a* and *b* vice versa. Whilst M_a and M_b is moment at load position with distance *a* and *b*.

Finally, three proposed model for the calculation of effective moment of inertia, I_e, of lightweight reinforced concrete beams are concluded in Table 6 below.

Table 6 Model proposed for each loading type.

Load condition	Model I_e proposed	Designation
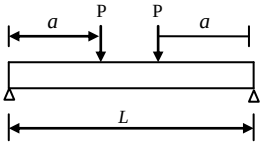	Applying Eq. (5), with Eq. (11) and Eq. (17)	M-1
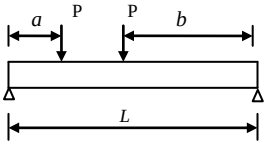	Applying Eq. (5) with Eq. (11) and Eq. (18)	M-2
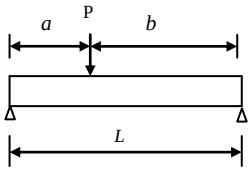	Applying Eq. (5) with Eq. (11) and Eq. (19)	M-3

5 Discussions of the Results

5.1 Symmetrical Two Points Load Acting on the Beam

The models proposed as given in Table 6 are verified using the data obtained from the beams tested in this study. The overall results from these experiments are presented to compare the actual and predicted deflections using existing model, Figure 5(a), and model proposed at serviceability load levels about 50% to 70 % of the ultimate load, $P_{u,}$ as shown in Figure 5(b).

From the figure, it is clear that the vast majority of calculated deflections using proposed model overestimated the measured values but within the range of 20 % error in which the limit is still acceptable [8]. However, the existing model predicts underestimated deflection with majority out of 20% error limit as shown in Figure 5(a).

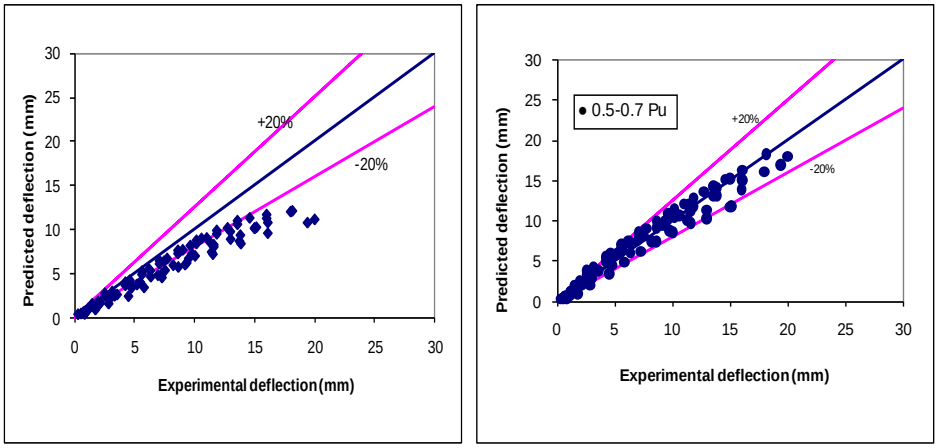

(a) Existing model **(b) Proposed model**

Figure 5 Comparison of measured and predicted deflection.

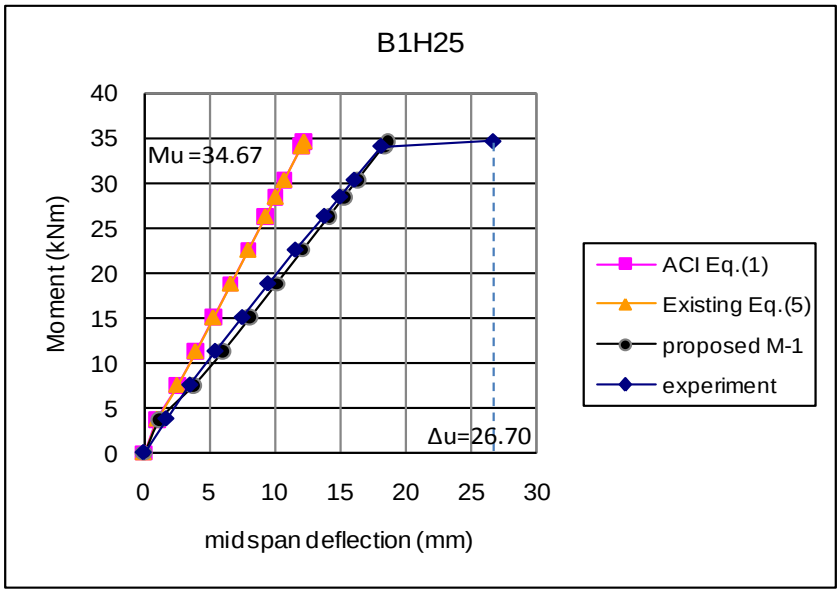

Figure 6 Typical deflection calculation using various models.

Figure 6 shows typical load-deflection curve for beam tested under two symmetrical points load. From the figure it can be seen that deflection predicted by ACI and the existing model, Eq. (5) with Eq. (6) and Eq. (7), give underestimate prediction to experimental values. Whilst model proposed in this study are agree well with the experimental value.

5.2 Beam under Asymmetrical Two Points Load

Again in this section, three model discussed previously are employed to calculate deflection for beams under asymmetrical points load as shown in Figure 7 below. The proposed model, M-2 in Table 6, give good prediction compare to experimental deflection. Whilst ACI and existing model are still underestimated the experimental value.

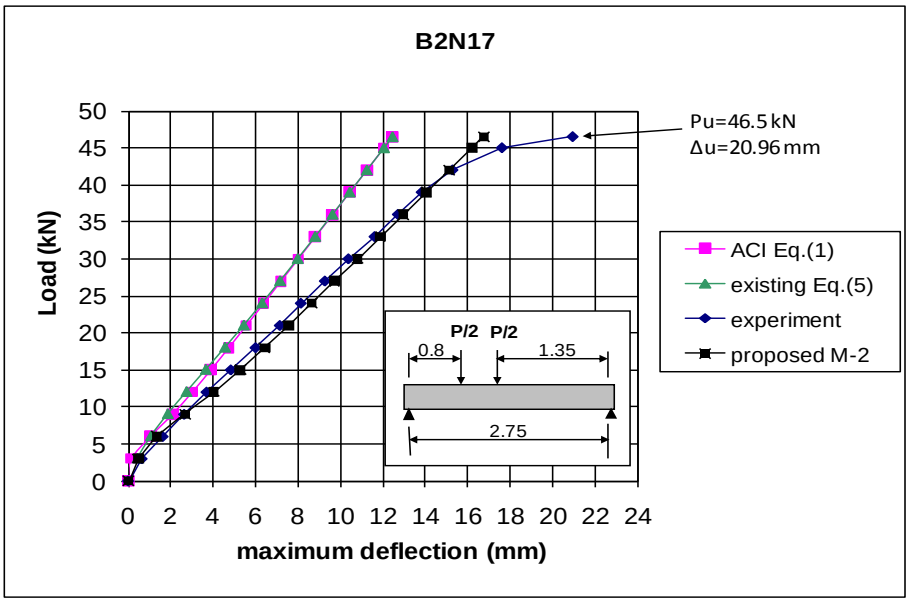

Figure 7 Typical deflection calculation using various models for asymmetrical two points load.

5.3 Beam Subjected to Single Point Load at Any Position

Proposed model M-3 given in this study is used to predict deflection of beam under single point load as shown in Figure 8. The results are presented alongside results produced by ACI and existing model. In the region of 30 to 60% of ultimate load ACI model give quite good prediction but still in underestimate prediction. However, at all load level the existing model produce underestimate deflection compare to the measured deflection. The proposed model again produces more accurate deflection prediction compare to the deflection predicted by the existing model.

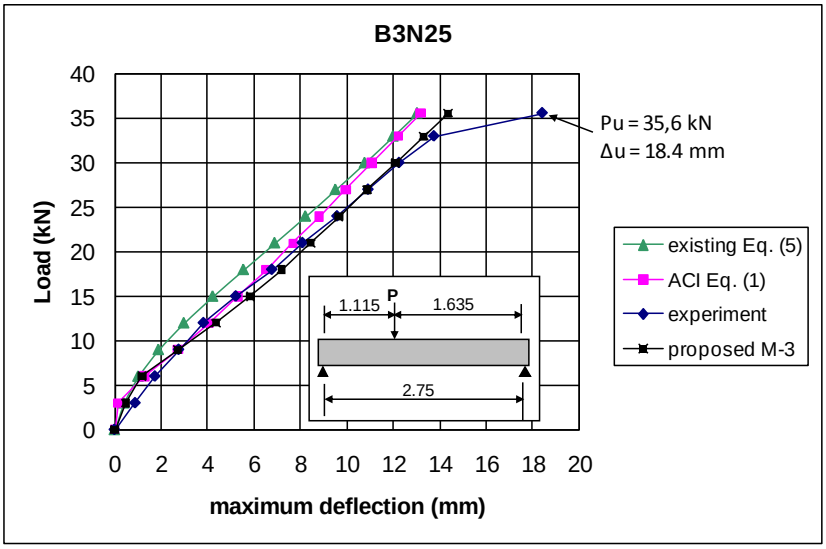

Figure 8 Comparison between measured and calculated deflection using various models for single point load at any position.

6 Conclusions

Three proposed models for calculating the effective moment of inertia by incorporating the effect of reinforcement ratio are introduced. The model proposed in this study are all agree with the experimental value and give better accuracy than the existing model and in some cases have similar trend with model proposed by the ACI code.

Acknowledgement

The author would like to thank Mr. Suparjo and Mr. Joedono, lecturer of Civil Engineering Department, University of Mataram, for warm discussions during the project. I would also like to gratefully acknowledge the financial support from Directorate General of Higher Education, Ministry of National Education.

References

[1] Sugiharto, H., Prasetyo, A., Ary, F., P., *Studi Penggunaan Batu Apung Untuk Beton Ringan Sebagai Komponen Struktural*, Laporan Penelitian No.01/Pen/SIPIL/1997, UK Petra, Surabaya, 1997.

[2] ASTM C330-89, *Standard Specification for Lightweight Aggregate for Struktural Concrete*, Annual Book of ASTM Standards, **4**(2), 1992.

[3] SNI 03-2847-2002, *Tata Cara Penghitungan Struktur Beton untuk Bangunan Gedung*, Badan Penerbit Pekerjaan Umum, Jakarta Selatan, 2002.
[4] Rossignolo, J.A. & Agnesini, M.V.C., *Durability of polymer-modified lightweight aggregate concrete*, Cement and Concrete Composite, **26**, pp. 375-380, 2004.
[5] Haque, M.N., Al-Khaiat, H. & Kayali, O., *Strength and Durability of Lightweight Concrete*, Cement & Composite Concrete, **26**, pp. 307-314, 2004.
[6] Owens, P.L., *Structural lightweight Aggregate Concrete-the Future*?, Concrete, **33**(10), pp. 45-7, 1999.
[7] ACI Committee 318, *Building Code Requirement for Reinforced Concrete and Commentary* (ACI 318-02/ACI 318R-02), American Concrete Institute, Detroit, pp. 103, 2002.
[8] Branson, D.E., *Instantaneous and Time dependent Deflection of simple and Continues Reinforced Concrete Beams*, HPR Report No. 7, Part 1, Alabama, Highway Department/US Bureau of Public Roads, pp 1-78, 1963.
[9] Al-Shaikh, A.H. & Al-Zaid, R.Z., *Effect of Reinforcement Ratio on the Effective Moment of Inertia of Reinforced Concrete Beams*, ACI Structural Journal, **90**(2), pp. 144-148, 1993.
[10] Al-Zaid, R.Z., Al-Shaikh, A.H. & Abu-Hussein, M.M., *Effect of Loading Type on the Effective Moment of Inertia of Reinforced Concrete Beams*, ACI Structural Journal, **88**, pp. 184-190, 1991.
[11] Ashour, S.A., *Effect of Compressive strength and Tensile Reinforcement ratio on flexural behaviour of high-strength concrete beams*, Engineering Structures, **22**, pp. 413-423, 2000.
[12] Ghali, A., *Deflection of Reinforced Concrete Members: A Critical Review*, ACI Structural Journal, **90**(4), July-August, 1993, pp. 364-373, 1993.
[13] Gilbert, R.I., *Deflection Calculation for Reinforced Concrete Structures-Why We Sometimes Get It Wrong*, ACI Structural Journal, **96**, pp. 1027-1032, 1999.
[14] Gilbert, R.I., *Shrinkage, Cracking and Deflection - the Serviceability of Concrete Structures*, Electronic Journal of Structural Engineering, **1**, pp. 15-37, 2001.
[15] Grossman, J.S., *Simplified Computations for Effective Moment of Inertia Ie and Minimum Thickness to avoid Deflection Computations*, ACI Structural Journal, **78**, pp. 423-439,1981.
[16] Fikry, A.M. & Thomas, C., *Development of a model for the effective moment of inertia of one-way reinforced concrete elements*, ACI Structural Journal, **95**(4), pp. 444-455,1998.

[17] Akmaluddin & Thomas, C., *Experimental Verification of Effective Moment of Inertia Used in the Calculation of Reinforced Concrete Beam Deflection*, Proceeding of Civil Engineering Conference "Towards Sustainable Civil Engineering Practice", Petra Christian University, Surabaya, pp. 89-98, 2006.

[18] Almussalam, A., Beshr, H., Maslehuddin, M. & Al-Amoudi, O., *Effect of Silica Fume on the Mechanical properties of Low quality Coarse Aggregate Concrete*, Cement & Composite Concrete, **26**, pp. 891-900, 2004.

[19] Campione, G. & Mendola, La L., *Behaviour in Compressions of Lightweight fibre Reinforced Concrete with Transverse Steel Reinforcement*, Cement & Composite Concrete, **26**, pp. 645-656, 2004.

[20] ASTM C39-86, *Standard Test Method for Compressive Strength of Cylindrical Concrete Specimens*, Annual Book of ASTM Standards, **4**(2), 1992.

[21] ASTM C-469, *Standard Test Method for Static Modulus of Elasticity and Poisson's Ratio of Concrete in Compression*, Annual Book of ASTM Standards, **4**(2),1992.

[22] Kuang, K.S.C., Akmaluddin, Cantwell, W.J. & Thomas C., *Crack Detection and Vertical Deflection Monitoring in Concrete Beams Using Plastic Optical Fibre Sensors*, Measurement Science and Technology, **14**, pp. 205-216, 2003.